Utah State University
DigitalCommons@USU

Space Dynamics Lab Publications | Space Dynamics Lab

1-1-2006

Retrieval of Physical Properties of Particulate Emission from Animal Feeding Operations Using Three-Wavelength Elastic Lidar Measurements

Vladimir V. Zavyalov

Christian Marchant

Gail E. Bingham

Thomas D. Wilkerson

Jason Swasey

Christopher Rogers

See next page for additional authors

Follow this and additional works at: https://digitalcommons.usu.edu/sdl_pubs

Recommended Citation

Zavyalov, Vladimir V.; Marchant, Christian; Bingham, Gail E.; Wilkerson, Thomas D.; Swasey, Jason; Rogers, Christopher; Ahlstrom, Douglas; and Timothy, Paul, "Retrieval of Physical Properties of Particulate Emission from Animal Feeding Operations Using Three-Wavelength Elastic Lidar Measurements" (2006). *Space Dynamics Lab Publications.* Paper 151.
https://digitalcommons.usu.edu/sdl_pubs/151

This Article is brought to you for free and open access by the Space Dynamics Lab at DigitalCommons@USU. It has been accepted for inclusion in Space Dynamics Lab Publications by an authorized administrator of DigitalCommons@USU. For more information, please contact digitalcommons@usu.edu.

Authors

Vladimir V. Zavyalov, Christian Marchant, Gail E. Bingham, Thomas D. Wilkerson, Jason Swasey, Christopher Rogers, Douglas Ahlstrom, and Paul Timothy

This article is available at DigitalCommons@USU: https://digitalcommons.usu.edu/sdl_pubs/151

Retrieval of physical properties of particulate emission from animal feeding operations using three-wavelength elastic lidar measurements

Vladimir V. Zavyalov, Christian Marchant, Gail. E. Bingham, Thomas D. Wilkerson, Jason Swasey, Christopher Rogers, Douglas Ahlstrom, and Paul Timothy

Space Dynamics Laboratory, 1695 North Research Parkway, North Logan, UT 84341

Tel: 435-797-4116 Fax: 435-797-4599 vladimir.zavyalov@sdl.usu.edu

ABSTRACT

Agricultural operations produce a variety of particulates and gases that influence ambient air quality. Lidar (LIght Detection And Ranging) technology provides a means to derive quantitative information of particulate spatial distribution and optical/physical properties over remote distances. A three-wavelength scanning lidar system built at the Space Dynamic Laboratory (SDL) is used to extract optical parameters of particulate matter and to convert these optical properties to physical parameters of particles. This particulate emission includes background aerosols, emissions from the agricultural feeding operations, and fugitive dust from the road. Aerosol optical parameters are retrieved using the widely accepted solution proposed by Klett. The inversion algorithm takes advantage of measurements taken simultaneously at three lidar wavelengths (355, 532, and 1064 nm) and allows us to estimate the particle size distribution. A bimodal lognormal particle size distribution is assumed and mode radius, width of the distribution, and total number density are estimated, minimizing the difference between calculated and measured extinction coefficients at the three lidar wavelengths. The results of these retrievals are then compared with simultaneous point measurements at the feeding operation site, taken with standard equipment including optical particle counters, portable PM_{10} and $PM_{2.5}$ ambient air samplers, multistage impactors, and an aerosol mass spectrometer.

Keywords: Remote sensing, lidar, aerosols, pollution, air quality

I. INTRODUCTION

The lidar technique has been successfully applied to qualitatively characterize particulate emissions from agricultural sources[1, 2]. Typical lidar systems employed for agricultural applications, however, are based on single wavelength lasers and have limited abilities to characterize particulate emission quantitatively. The Space Dynamics Laboratory (SDL) at Utah State University has teamed with ARS researchers to build a three-wavelength lidar system for remote sensing of pollution from agriculture activities. The aerosol backscatter cross section is uniquely determined by the physical and chemical properties of the aerosols (size, shape, and complex refractive index) and the laser wavelength. The wavelength dependence of the backscatter coefficient is mainly determined by the aerosol size distribution and refractive index. Using backscatter coefficients measured at several laser wavelengths, the physical properties of aerosols can be retrieved using the inverse solution of the Mie integral equations[3]. Thus a multiwavelength lidar system can provide not only information on the 3D distribution of particulate matter, but also information on the particulate size distribution in a 3D space with the ability to convert this information to the standard EPA (Environmental Protection Agency) mass concentration units like PM_{10}, $PM_{2.5}$, PM_1 and PM_{10}-$PM_{2.5}$.

Aerosol sounding techniques for the retrieval of physical aerosol parameters from multi-wavelength lidar measurements have been developed since the 1980s and have made major progress in the past five years[3-6]. Unambiguous and stable retrieval of the physical parameters of aerosols requires measurements of backscatter coefficients for at least three laser wavelengths and the aerosol extinction coefficient for at least two wavelengths using additional Raman channels[3, 5, 6]. From the instrumental point of view, multi-wavelength lidar systems with additional

Remote Sensing of Aerosol and Chemical Gases, Model Simulation/Assimilation, and Applications to Air Quality, edited by Allen Chu, James Szykman, Shobha Kondragunta, Proc. of SPIE Vol. 6299, 62990S, (2006)
0277-786X/06/$15 · doi: 10.1117/12.680967

Downloaded From: http://proceedings.spiedigitallibrary.org/ on 04/02/2015 Terms of Use: http://spiedl.org/terms

Raman channels are still very expensive and complicated to operate. A three-wavelength lidar system appears to be a reasonable tradeoff between accurate and stable retrievals, and the ability to operate under different environmental conditions with minimal measurement time. To date, a significant data base of atmospheric aerosol characteristics has been obtained by the combination of satellite and ground based observations[4, 7]. Using this database, research has shown that the physical properties of assumed aerosols can be successfully retrieved based on measurements of backscatter coefficients of only three wavelengths [4, 8].

In this paper, we describe the retrieval algorithm and present initial results of the particulate emission characterization obtained by simultaneous remote measurements with a 3-wavelength lidar and in situ point particulate measurements, performed with standard EPA approved equipment. Particulate chemical and physical properties measured in situ are used to make assumptions of the complex refractive index and the type/shape of the particle size distribution of particulate emissions present at the experiment site. They are used also to constrain the inverse solution to minimize overall errors and uncertainties in the lidar measurements. In situ measurements are used to calibrate and verify the results of the lidar retrievals as well. The experiment was conducted at a deep-pit swine production facility situated near Ames, in central Iowa, for approximately three weeks in August and September of 2005.

2. EMPLOYED INSTRUMENTATION AND EXPERIMENT SETUP

The AGLITE lidar instrument used in this study is a three-wavelength lidar system, designed and constructed at SDL under contract from the ARS. A single diode-pumped Nd:YAG laser, operating simultaneously at three wavelengths (1.064 μm, 0.532 μm, and 0.355 μm) with the high repetition rate of 10 kHz , is used as a transmitter of short impulses of radiation. The backscattered radiation is collected by a 28-cm Newtonian telescope with a full field of view (FOV) of 0.46 mrad. A beam-separation unit is used to split up the return backscattered light at three different channels. A photon counting system detects low return signals simultaneously for each channel. Interference filters are placed in front of each detector to suppress background daylight radiation from the atmosphere and optical cross talk between channels. The data from the photon counting unit are read out by the digital processing unit, averaged across a predetermined set of laser pulses, displayed in a real time, and stored /transmitted for further processing. The lidar system was optimized for eye safe operation at all three wavelengths at ranges from 0.5 to 15 km, with a minimum range resolution of 4.8 m. Technical details of the lidar design and construction are described by Wilkerson[9].

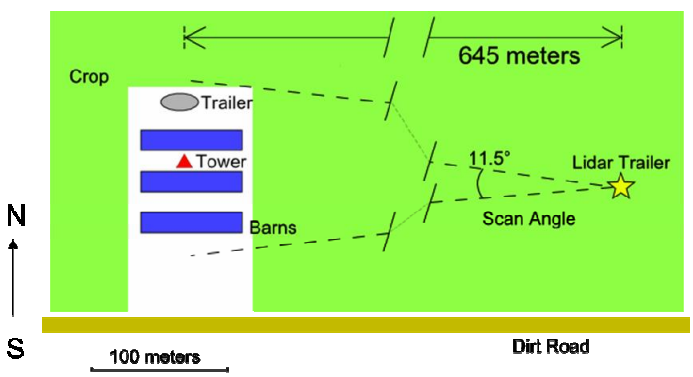

Fig. 1. Experimental site layout.

A schematic diagram of the deep-pit swine production facility and instrumentation employed on this site is shown in Fig. 1. The facility consisted of three separate parallel barns, each barn housing around 1250 pigs. A number of MetOne Optical Particle counters (OPC) 9722 were employed around this hog facility to provide information on particle size distribution from 0.3 to 10 μm in diameter in a real time. To measure chemical composition, the Aerodyne Aerosol Mass spectrometer (AMS) was deployed at the trailer. Portable $PM_{10}/PM_{2.5}$ (AirMetrics MiniVol) samplers were arrayed vertically and horizontally, and data were collected on a daily-averaged basis. A monitoring Davis weather station was established approximately 40 m to the north of the nearest barn to record the typical suite of meteorological parameters.

Downloaded From: http://proceedings.spiedigitallibrary.org/ on 04/02/2015 Terms of Use: http://spiedl.org/terms

3. INVERSION OF THE LIDAR SIGNAL

3.1 Theoretical development

The logarithmic range normalized lidar return power S=$S(R, \lambda)=ln[P(R,\lambda)\cdot R^2]$ for two distinct classes of scatterers may be written in the form[10]:

$$S = \ln(C \cdot P_0) + \ln(\beta_b + \beta_a) - 2\int_0^R (\alpha_b + \alpha_a) dR' \tag{1}$$

Where P (R, λ) is the lidar return power from the range R. C=$F\cdot\xi\cdot A_0\cdot\Delta R$ is the lidar calibration constant. The term F represents the losses in the transmitting and receiving optics, ξ= ξ (R,λ) represents the lidar overlap geometrical form factor, A_0 represents the effective telescope area, and the range increment ΔR of the lidar is defined as τ·c/2, the product of the effective laser pulse duration τ and speed of light c. The term $P_0=P_0(\lambda)$ is the laser pulse power transmitted at wavelength λ. The terms $\beta_b=\beta_b(R,\lambda)$ and $\beta_a=\beta_a(R,\lambda)$ represent the backscatter coefficients of air molecules and aerosol particles respectively. The terms $\alpha_a=\alpha_a(R,\lambda)$ and $\alpha_b=\alpha_b(R,\lambda)$ are extinction coefficients of aerosols and air molecules correspondingly.

Typically, the molecular part of Eq. (1) can be calculated using standard atmosphere conditions at different altitudes[5]. Aerosol backscatter and extinction coefficients are two unknowns in a single lidar equation. The standard solution of this equation involves two *a priori* assumptions or constraints. The first assumption is the relationship between aerosol extinction and backscatter coefficients L (lidar ratio):

$$L = \frac{\alpha}{\beta} \tag{2}$$

The second assumption is that boundary conditions must be defined for Eq. (1). This is done by determining a reference value of either the extinction coefficient $\alpha_D = \alpha_a(\lambda, R_D) + \alpha_b(\lambda, R_D)$, or the backscatter coefficient. This value is independently measured at the reference range R_D, either using a separate retrieval technique on the lidar data, or using a completely separate in situ instrument. With these constraints, Eq. (1) can be solved analytically. Following Klett's standard solution for two distinct scatters[10], the aerosol backscatter coefficient can be solved for from Eq. (1) at each laser wavelength λ separately:

$$\beta_a = \frac{e^{\left[S'(R) - S'_D\right]}}{\left(\frac{\alpha_{aD}}{L_a} + \frac{\alpha_{bD}}{L_b}\right)^{-1} + 2\int_R^{R_D} L_a e^{\left[S'(R') - S'_D\right]} \partial R'} \tag{3}$$

Where the term S_D is defined as $S_D= S(\lambda,R_D)$ and variables S' and S'_D are defined in terms of the S function as following:

$$S' - S'_D = S - S_D - 2L_b \int_R^{R_D} \beta_b \partial R' + 2\int_R^{R_D} L_a \beta_b \partial R' \tag{4}$$

The subscript "D" refers to a variable value measured at the reference range R_D. Note that signs before the third and fourth terms in Eq.(4) are mistakenly inverted in the Klett's original paper and are correct in the Eq.(5). The original solution (3) was derived for typical atmospheric applications when a lidar system is looking straight up, so that the molecular contribution is significant for altitudes above the aerosol boundary layer. For agricultural applications, measurements are conducted close to ground level and the main contribution to atmospheric scattering is from aerosols, while the molecular contribution is negligibly small. In this case we are still dealing with two distinct types of scatterers such as background aerosols and a pollutant. For this application, Eqs.(1-4) are still valid and we attribute the subscript "b" to the atmospheric background aerosols while the subscript "a" will refer to the particulate emission, the properties of which we seek to retrieve.

Downloaded From: http://proceedings.spiedigitallibrary.org/ on 04/02/2015 Terms of Use: http://spiedl.org/terms

For an optically thin pollutant cloud, the backscatter coefficient of the pollutant can be estimated directly from the lidar return signal, avoiding Klett's solution (3) and the assumptions that it requires. A schematic diagram of this method is presented in Fig. 2b. If the reference range is located beyond the pollutant, subtracting the signal S_D at the reference range R_D from signal S_a at the pollutant measurement point R_a, we can write:

$$S_a - S_D = \ln\left(\frac{\beta_a + \beta_b}{\beta_b}\right) - 2\int_{R_D}^{R_a} (\alpha_b + \alpha_a)\partial R' \approx \ln\left(\frac{\beta_a + \beta_b}{\beta_b}\right) - 2\int_{R_D}^{R_a} \alpha_b \partial R' \tag{5}$$

For the case of an optically thin pollutant cloud, the integral of the extinction term σ_a has a negligible effect on the signal and can be ignored. Rearranging this equation results in

$$\beta_a \approx \beta_b \exp\left(S_a - S_D + 2\int_{R_D}^{R_a} \alpha_b \partial R'\right) - \beta_b \tag{6}$$

Agricultural pollutant clouds are typically spatially localized around an emission source and particulate concentrations only slightly exceed the background aerosol loading so that backscatter values estimated by this approximation method agree well with Klett's retrievals. In our retrieval algorithm, we use this approach as a first guess to estimate the lidar ratio (2) for pollutant.

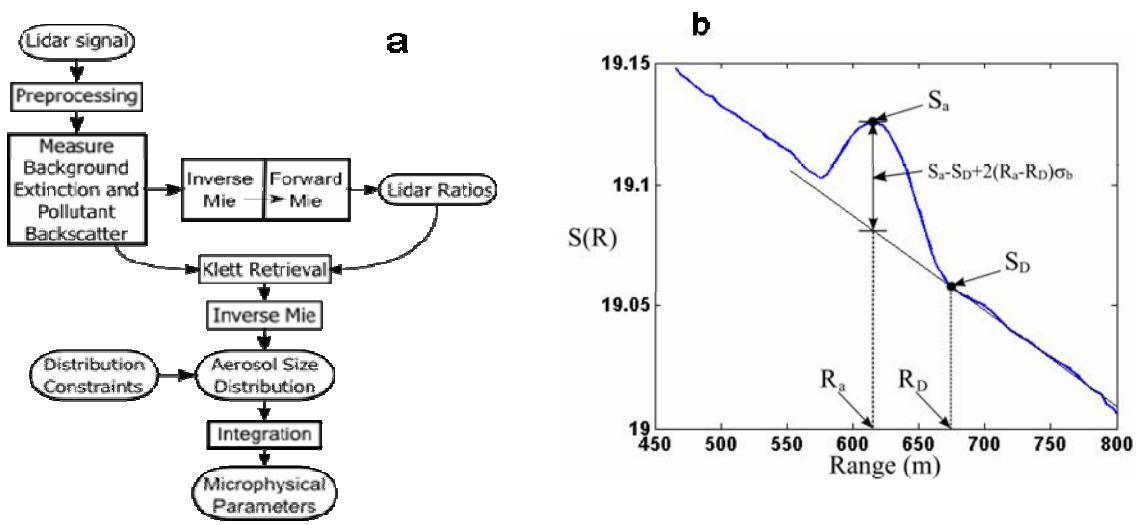

Fig. 2. Retrieval algorithm flow chart (a) and schematic diagram of estimation of the backscatter coefficient in the pollutant cloud (b).

To retrieve the parameters of the particle size distributions for background and particulate aerosols, the inverse Mie solution has been developed. Based on the OPC data measured in situ, we approximate the particle size distribution as a bimodal lognormal distribution for both accumulation and coarse particle modes (j=1, 2):

$$n(r) = \sum_{j=1}^{2} \frac{N_j}{\sqrt{2\pi} \cdot r \cdot \ln \sigma_j} \cdot \exp\left[\frac{1}{2}\left(\frac{\ln r - \ln r_{\mathrm{mod}\,N,j}}{\ln \sigma_j}\right)^2\right] \tag{7}$$

For any mode j of the distribution, N_j is the total number of particles in the given mode, $r_{\mathrm{mod}\,N,j}$ is the mode radius, and σ_j measures the width of the given mode. To estimate the mode radius and particle number densities N_j, we are using a modified version of the minimization technique described by Del Guasta[8].

In general, the inverse Mie algorithm works by estimating the optical parameters associated with a set of aerosol particle size distribution parameters and by minimizing the difference between the estimated and the measured optical parameters. First, appropriate ranges are selected for the parameters of the particle size distribution. This defines a space

Downloaded From: http://proceedings.spiedigitallibrary.org/ on 04/02/2015 Terms of Use: http://spiedl.org/terms

of possible particle size distributions. Then, a vector of optical parameters is calculated for each point in the particle size distribution space, forming a space of estimated possible optical parameters. Finally, the estimated optical parameter vector that is closest to the measured optical parameter vector is selected, and the algorithm returns the corresponding particle size distribution.

The relationship between the particle size distribution and the optical parameters of an aerosol are defined by Mie scattering theory. The Mie equations[3] for extinction and backscatter are as follows:

$$\begin{aligned} \alpha(r,\lambda) &= \int \pi r^2 Q_{ext}\left(r,m,\lambda\right) n\left(r\right) \partial r \\ \beta(r,\lambda) &= \int \frac{1}{4} r^2 Q_{\pi}\left(r,m,\lambda\right) n\left(r\right) \partial r \end{aligned} \tag{8}$$

Where Q_{ext} and Q_{π} are Mie extinction and backscatter efficiencies respectively. A bimodal lognormal distribution is described by a total of six parameters (six-dimensional solution space). Since the inversion of a vector of extinction values requires estimating the corresponding extinction values for each possible particle size distribution, this makes the problem potentially intractable. The bimodal lognormal distribution can be written as a linear combination of two particle normalized distributions by bringing the particle number count coefficient N_j outside of the equation. Let the term $\tilde{n}_j\left(r\right)$ represent the jth mode of the particle size distribution, normalized for a single particle.

$$n\left(r\right) = \sum_{j=1}^{2} N_j \tilde{n}_j\left(r\right) \tag{9}$$

Considering the case for extinction and substituting Eq. (9) into Eq. (8), particle normalized extinction values can be calculated for each particle normalized mode of the particle size distribution. If a vector is formed of extinction values at each wavelength, this vector can be expressed as a linear combination of particle normalized extinction values.

$$\begin{aligned} \tilde{\alpha}_{j\lambda} &= \int \pi r^2 Q_{ext}\left(r,m,\lambda\right) \tilde{n}_j\left(r\right) \partial r \\ \boldsymbol{\alpha} &= \begin{vmatrix} \alpha_{1,UV} & \alpha_{2,UV} \\ \alpha_{1,V} & \alpha_{2,V} \\ \alpha_{1,IR} & \alpha_{2,IR} \end{vmatrix} \begin{vmatrix} N_1 \\ N_2 \end{vmatrix} = A\mathbf{n} \end{aligned} \tag{10}$$

Let a weighted norm be defined for the space of optical parameter vectors.

$$\left|\boldsymbol{\alpha}\right|^2 = \boldsymbol{\alpha}^T W \boldsymbol{\alpha} = \sum_{j=1}^{3} w_j \alpha_j^2 \tag{11}$$

The signal to noise ratio is used to form a weighting matrix W in order to account for different noise levels at each wavelength. It is possible to analytically determine the values of the particle number count coefficients that minimize the error between the measured and estimated extinction vectors. This is done by taking the gradient of the error with respect to **n** and setting it equal to the zero vector. Let the vector of measured extinction values be denoted by $\boldsymbol{\alpha}$ and the vector of estimated extinction values be denoted by $\hat{\boldsymbol{\alpha}}$.

$$\begin{aligned} \left|\boldsymbol{\alpha} - \hat{\boldsymbol{\alpha}}\right|^2 &= \left(\boldsymbol{\alpha} - A\hat{\mathbf{n}}\right)^T W \left(\boldsymbol{\alpha} - A\hat{\mathbf{n}}\right) \\ \frac{\partial}{\partial \mathbf{n}} \left|\boldsymbol{\alpha} - \hat{\boldsymbol{\alpha}}\right|^2 &= \mathbf{0} = -A^T W \boldsymbol{\alpha} + A^T W A \hat{\mathbf{n}} \\ \hat{\mathbf{n}} &= \left(A^T W A\right)^{-1} A^T W \boldsymbol{\alpha} \end{aligned} \tag{12}$$

Downloaded From: http://proceedings.spiedigitallibrary.org/ on 04/02/2015 Terms of Use: http://spiedl.org/terms

We recognize this solution as being the Moore-Penrose pseudo-inverse[15] for a weighted inner product. This solution allows us to analytically determine the particle number count coefficients, given the remaining aerosol parameters. This procedure can also be applied to a distribution with an arbitrary number of modes.

Each particle normalized extinction value $\tilde{\alpha}_{j\lambda}$ is a function of μ_{modj} and σ_j for the jth mode of the particle size distribution. The matrix $\boldsymbol{A}$ is therefore a function of these parameters of each of the modes of the particle size distribution. Let the set of possible aerosol parameters $[\mu_1,\mu_2,\sigma_1,\sigma_2]$ be denoted by **s**. The estimate of the particle number count vector corresponding to that set can be written as

$$\hat{\mathbf{n}} = \left(A_s^T W A_s\right)^{-1} A_s^T W \boldsymbol{\alpha} \tag{13}$$

The set $\hat{\mathbf{s}}$ that is closest to the parameters of the true particle size distribution can be determined by varying the aerosol parameters and computing the value of the minimization function for each set of values. External constraints can be imposed on the solution by fixing the value of some of the elements of **s**. The error function is now defined as:

$$\varepsilon = \left|\boldsymbol{\alpha} - A_{\mathbf{s}}\hat{\mathbf{n}}\right|^2 \tag{14}$$

3.2 Retrieval algorithm

The retrieval of aerosol physical parameters from a raw lidar signal involves several major steps. The flow chart of the retrieval algorithm is shown in Fig. 2a. At the first preprocessing step, the geometrical form factor of the telescope receiving optics and scattered sunlight background radiation are estimated. The geometrical form factor in Eq. (1) takes into account the overlap between the transmitted laser beam and the FOV of the telescope receiving optics with a central obstruction. To calculate the geometrical form factor, the polynomial regression method for an inhomogeneous atmosphere proposed by Dho[11] is used. During daylight observations, the background radiation of sunlight scattered by the atmosphere dominates the lidar return signal at long distances. For each lidar measurement, this background radiation is approximated by least squares fitting to a constant value at distances of 5-15 km. The estimated background is then subtracted from the total lidar return signal.

The second step determines the backscatter at the background reference point $R=R_D$, as well as the lidar ratios of the background and the pollutant aerosols. The slope method is used to estimate background extinction coefficient at the far end of the particulate cloud. In close proximity to the emission source, the background aerosol loading is typically homogeneous and a standard slope method can be applied (see Fig. 2b). For each wavelength, the slope of a line that has been fit in a least-squares sense to the curve S(R) is used as an estimate of $\alpha_b(\lambda, R)$:

$$\alpha_b = -2\frac{dS}{dR} \tag{15}$$

This value is then used in Klett's solution (3) as a reference value $\alpha_{aD} = \alpha_{bD}$ at the far end of pollutant cloud $R=R_D$.

In order to estimate the lidar ratio of the pollutant we are using the approximation method described above by Eqs. (5) and (6) to estimate the backscatter coefficient inside of the cloud. After the background extinction and pollutant backscatter coefficients have been estimated, the lidar ratios for both pollutant and background aerosols are calculated using the inverse and forward Mie solutions. At this retrieval step, the inverse Mie solution is used as an estimate of the parameters of a bimodal lognormal particle size distribution (7) for both background aerosols and particulate emission at a point in the middle of the pollutant cloud. Knowing the particle size distribution, the backscatter and extinction values for background and particulate aerosols are estimated using forward Mie calculations, Eqs. (8), which are in turn used to determine the lidar ratios (2).

The third step is to retrieve backscatter values for the entire data set. Lidar ratios and the backscatter coefficient β_D at the reference point are then substituted into Klett's solution (3), and range dependent backscatter coefficients are calculated over the entire range of the pollutant cloud for all three wavelengths. Using this approach, all optical parameters (backscatter and extinction coefficients and thus the lidar ratio) of the background and particulate aerosols are calculated in a few retrieval steps at all three lidar wavelengths.

Downloaded From: http://proceedings.spiedigitallibrary.org/ on 04/02/2015 Terms of Use: http://spiedl.org/terms

The final step is to convert the backscatter values of the entire data set into microphysical parameters of background and pollutant aerosols. The inverse Mie solution described previously is used to calculate the parameters of a bimodal particle size distribution (7) for particulate cloud at each range bin. External constrains can be imposed on the minimization solution by fixing parameters of the particle size distribution at specific values. These parameters can be estimated from particle size distributions measured in situ with OPC and AMS sensors. Once the parameters of particle size distribution and total number densities are estimated, the mass concentration of particles with different size range can be easily calculated using in situ measurements of particulate chemical composition and density. This final step is denoted as integration in Fig. 2a.

3.3 Particle size distribution

Proper conversion of lidar data involves the construction of a model of the particulate composition and size distribution based on in-situ measurements. The chemical composition of background aerosols and particulate emission from hog barns was estimated using in situ data from the AMS and chemical analysis of particulate mass sampled with AirMetric ambient air samplers. Chemical analysis[12] has shown that both background and pollutant aerosols are composed mostly of sulfate, nitrate, ammonium, and organic carbon. These compounds are consistent with the makeup of typical atmospheric water-soluble aerosols detailed in OPAC[13] and the Air Force[14] atmospheric aerosols databases. We approximated the optical properties of both background and pollutant aerosols by those of water–soluble atmospheric aerosols. Following the OPAC database we also assumed that fugitive dust is composed of a mixture of quartz and clay materials. Values of the complex refractive index $\boldsymbol{m}$ for water-soluble and dust-like aerosols were selected from the *Handbook of Geophysics and the Space Environment* [14].

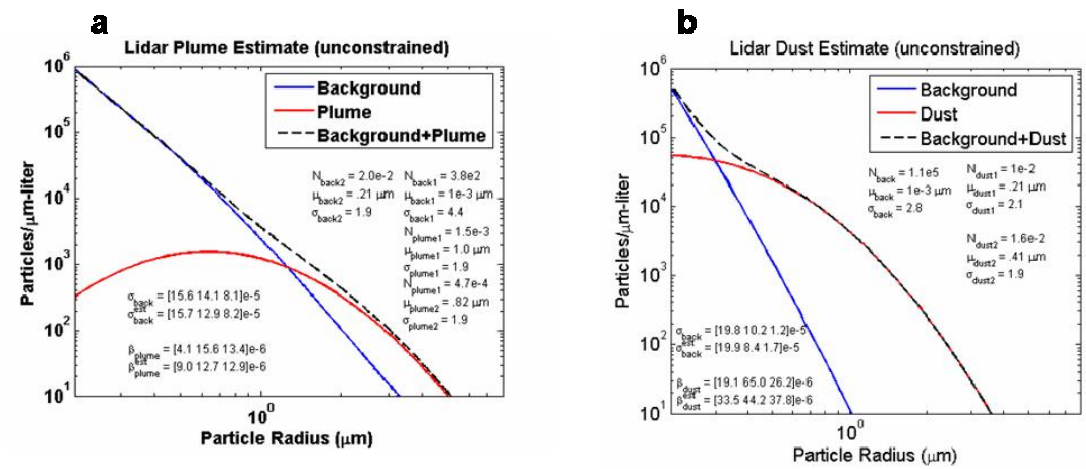

Fig. 3. Particle size distribution for particulate emission (a) and fugitive dust cloud (b) retrieved from the 3-λ lidar data with no constraints.

The bimodal particle size distribution (7) is described by six independent parameters. In addition, the Mie equations (8) require an additional three complex variables for the index of refraction, leaving a total of nine independent parameters to describe the aerosol, while only three lidar measurements are available for inversion. To reduce the number of the variables involved, we assumed the refractive index of aerosol to be constant, and additionally applied various constraints on the parameters of particle size distribution. In Figs. 3-4 we demonstrate particle size distributions retrieved for particulate and fugitive dust clouds (graphs a and b, respectively) under different constraints. Fig. 3 demonstrates the unconstrained inverse Mie solution (six retrieved parameters). In Fig. 4 the mode radius $\boldsymbol{\mu}$ and width of the distribution $\boldsymbol{\sigma}$ are fixed for both modes, and only two quantities (total number densities in fine and coarse modes) are retrieved. To constrain the parameters of particle size distribution, the combined OPC and AMS data measured in situ were used. The particle size distribution retrieved from the three-wavelength lidar data is compared to the combined OPC-AMS distribution for particulate emission in Fig. 4a and fugitive dust events in Fig. 4b.

Downloaded From: http://proceedings.spiedigitallibrary.org/ on 04/02/2015 Terms of Use: http://spiedl.org/terms

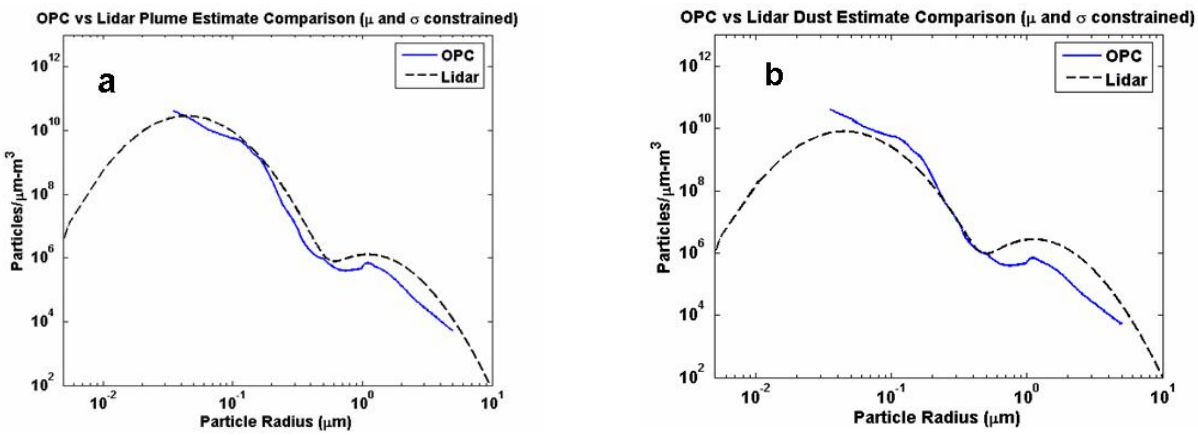

Fig. 4. Comparison of particle size distribution measured by OPC sensor and retrieved from the lidar data with **μ**- and **σ** constraints for particulate emission (a) and fugitive dust (b).

It has been found that the ***μ***-constrain (or **σ**-constrain) distribution tends to decrease the width and contribution of the coarse particle mode. The unconstrained solution tends to converge to a single mode distribution (see Fig. 3). When both mode radius and width of the distribution are fixed, the lidar retrievals are in a good agreement with particle size distribution measured in situ with OPC-AMS sensors for both particulate emission and dust events (see Fig. 4).

4. EXPERIMENTAL RESULTS AND DISCUSSION

An extended series of lidar observations were conducted during three weeks of field campaign at the deep-pit swine production facility. Typical lidar scan patterns include vertical scans between barns and on any side of the barns and sensor trailer, horizontal scans above the barns, stationary time series scans of particulate emission in close proximity to the in situ instrumentation, and any combination of vertical and horizontal scans. Two dirt roads bordered the swine production facility. Occasional traffic along both roads caused extensive fugitive dust traveling from the roads over the swine facility. These events were captured during lidar operations as well.

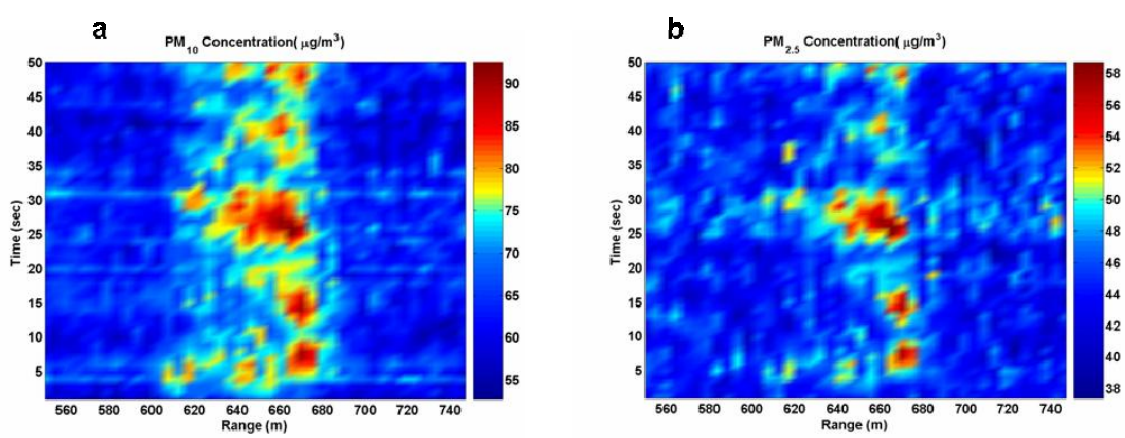

Fig. 5. 2D images of particulate mass concentrations PM_{10} (a) and $PM_{2.5}$ (b) retrieved from the lidar time series at the middle of the tower.

Downloaded From: http://proceedings.spiedigitallibrary.org/ on 04/02/2015 Terms of Use: http://spiedl.org/terms

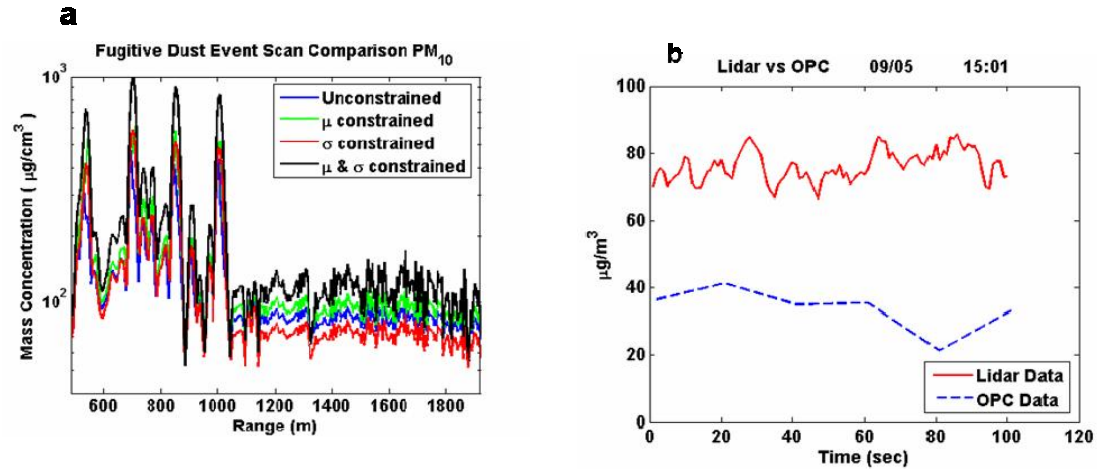

Fig. 6. a) Fugitive dust mass concentration PM_{10} retrieved from the lidar data under different constraints. b) Comparison of mass concentration PM_{10} measured by the OPC in the middle of the tower and by the lidar in the middle of pollutant cloud collocated with the OPC (see image in Fig. 5a).

The ability of the lidar system and algorithm to retrieve particulate concentration at a level comparable with the natural variability of background aerosols is demonstrated in Fig. 5 and Fig.6b. Particulate mass concentrations PM_{10} and $PM_{2.5}$ are retrieved from the lidar time series measurements taken in the middle of the central tower. Mass concentration PM_{10} estimated from the lidar signal is compared with in situ measurements by the OPC in Fig. 6b. Both measurements represent a time series of particulate emission measured simultaneously at the middle of the central tower. It is seen that particulates were being emitted from barns at 5-10 second intervals. The lidar accumulation time was set to 1 second while the accumulation time of the OPC sensors was 20 seconds so that the OPC counts represent a time average of periodic events. According to the lidar measurements, the peak concentration of particulate emission is only ~30% higher than the background aerosol mass concentration while the mean particulate emission exceeded the background by only ~14%.

The results of the retrievals during fugitive dust events are shown in Fig. 6a. The dust mass concentration for PM_{10} has been calculated from particle size distributions estimated with different constraints. It is seen that different distributions give mass concentration PM_{10} varying up to two times. To choose the right distribution (constraint), this data have to be validated against in situ measurements with the OPC and PM-sampler instrumentation.

For absolute calibration and validation of any retrieval quantity, reliable truth data must be acquired under the same measurement conditions. For truth data in this experiment we are using AirMetric portable PM_{10} and $PM_{2.5}$ samplers placed at different locations around the hog farm. The background, non-barn influenced PM_{10} and $PM_{2.5}$ concentrations were found to average around 37.4 ± 5.4 μg/m^3 and 11 ± 5.4 μg/m^3, respectively. In plume values measured at the central tower and sensor trailer varied within wide ranges, 40-70 μg/m^3 and 11-18 μg/m^3 respectively.

Three lidar time series measurements were averaged. The background aerosol mass concentration averaged around 61.9 μg/m^3 PM_{10} with an RMS uncertainty of ± 3.6 μg/m^3 and 34.2 ± 2.5 μg/m^3 of $PM_{2.5}$ The mean concentration of pollutant in the pollution plume was estimated in the middle of the plume cloud (as in Fig.6b) and averaged around 76.8 ± 5.6 μg/m^3 (PM_{10}) and 38.8 ± 3.5μg/m^3 ($PM_{2.5}$). These mass concentrations are about 40-70% higher than corresponding AirMetrics sampler data for both background and pollution aerosols.

Systematic analysis of the lidar retrieval process has shown that the biases are mostly induced by the reference value of background extinction coefficient estimated by slope method for Klett's inversion (3). The slope method gives excellent results for homogeneous atmosphere when background aerosol loading is uniform along the large portion of the lidar range. In real life, however, most of the measurements are made with elevation angles 1^0 -6^0 so that atmospheric homogeneity extends for only 50-250 m beyond the pollutant cloud due to height dependent aerosol loading.

Downloaded From: http://proceedings.spiedigitallibrary.org/ on 04/02/2015 Terms of Use: http://spiedl.org/terms

There are several ways to overcome this problem. First, additional reference lidar measurements at different elevations can be taken in relatively homogeneous atmosphere away from the particulate cloud to measure reference values for background aerosols using the slope method. Second, the reference values for background extinction coefficients can be estimated from in situ OPC data and used in retrievals as the direct reference value in Eq.(3) or as a constraint value for the slope method. Third, a simple scaling factor can be applied to the retrieved quantities as a calibration parameter. A bias in the background backscatter coefficient determined with the slope method gives a relative bias in the backscatter value for the pollutant cloud, which in turn leads to the relative bias in number concentration N_j of the particle size distribution (7), and thus in the estimated mass concentration. This calibration factor can be easily determined through time averaging of the lidar data and then relating them to AirMetrics sampler data.

6. CONCLUSION

A three-wavelength portable scanning lidar system has been developed at SDL to derive information of particulate spatial distribution and optical/physical properties of aerosols over remote distances. Preliminary results discussed in this paper have shown the great potential of remote lidar measurements taken at three wavelengths to characterize particulate emission quantitatively and represent spatial and temporal variations of the emitted plume as 3D/2D- mass concentration fields. To the best of our knowledge, this is the first attempt to characterize the agricultural emission sources as concentration fields of particulate masses such as PM_{10}, $PM_{2.5}$, PM_{10}-$PM_{2.5}$, and PM_1 applicable to the EPA regulation practices. The use of optical parameters derived from lidar measurements at three laser wavelengths, followed by a minimization solution was found to be a promising method for retrievals of the size distribution of any particulate emission present in the field. The strength of lidar returns from different particulate emissions varied by an order of magnitude, and the inversion algorithm developed to process three-wavelength lidar data gives meaningful results for all sources of particulate emissions.

The retrievals of mass concentration of background aerosols and particulate emission from the feeding operations agree within an order of magnitude with in situ measurements performed with PM_{10} and $PM_{2.5}$ ambient samplers. The main uncertainties involved are due to the incomplete knowledge of the parameters of particle size distribution used to constrain the iterative minimization technique. It has been shown that unconstrained solutions tend to converge into a single lognormal distribution. When mode radius and width of the distribution are used to constrain the inverse solution in both fine and coarse particulate modes, good agreement between lidar retrievals and OPC/ambient sampler data is achieved.

It is shown that biases in absolute mass concentrations retrieved from the lidar data are induced mainly by error in the reference value of background extinction coefficient extracted from the lidar signal itself. The slope method used in this work does not give a reliable and consistent reference value in real field conditions due to heterogeneity of atmospheric conditions surrounding the agricultural facility. Several methods are proposed to overcome this problem that need to be carefully investigated and tested under field conditions. In the meantime, a simple correction procedure is proposed to find a calibration factor for the lidar mass concentration retrievals. Future experiments are planned to test the proposed hypotheses and to develop an optimal strategy and protocols to verify, calibrate, and validate the results of three-wavelength lidar measurements.

ACKNOWLEDGEMENTS

The development of the AGLITE system was performed under USDA Agreement number 58-3625-4-121 with Dr. Jerry Hatfield, the Director of the National Soil Tilth Laboratory in Ames, Iowa, providing valuable direction to the AGLITE development team. Any opinions, findings, conclusions, or recommendations expressed in this publication are those of the authors and do not necessarily reflect the view of the U.S. Department of Agriculture.

REFERENCES

1. Holmen B.A., W.E. Eichinger, and R.G. Flocchini, "Application of elastic lidar to PM10 emissions from agricultural nonpoint sources", *Environ. Sci. Technol*. 32, 3066-3076 (1988).

Downloaded From: http://proceedings.spiedigitallibrary.org/ on 04/02/2015 Terms of Use: http://spiedl.org/terms

2. Stoughton T. E., D.R. Miller, "Vertical dispersion in the nocturnal, stable layer above a forest canopy", *Atmospheric Environment*. 35, 3989-3997 (2002).

3. Bockmann C, "Hybrid regularization method for ill-posed inversion of multiwavelength lidar data in the retrieval of aerosol size distributions", *Appl. Opt*. 40, 1329–1342 (2001).

4. Rajeev K. and K. Parameswaran., "Iterative method for the inversion of multiwavelength lidar signals to determine aerosol size distribution", *Appl. Opt*. 37. 4690–4700 (1998).

5. Bockmann C. , U. Wandinger, A. Ansmann, J. Bosenberg, V. Amiridis, A. Boselli, A. Delaval, F. De Tomasi, M. Frioud, I.V. Grigorov, A. Hagard, M. Horvat, M. Iarlori, L. Komguem, S. Kreipl, G. Larcheveque, V. Matthias, A. Papayannis, G. Pappalardo, F. Rocadenbosch, J. A. Rodrigues, J. Schneider, V. Shcherbakov, and M. Wiegner.. "Aerosol lidar intercomparison in the framework of the EARLINET project. 2. Aerosol backscatter algorithms", *Appl. Opt*. 43, 977-989 (2004).

6. Althausen D., D. Muller, A. Ansmann, U. Wandinger, H. Hube, E. Clauder, and S. Zorner, "Scanning six-wavelength eleven channel aerosol lidar", *J. Atmos. Ocean. Technol*. 17, 1469–1482 (2000).

7. Dubovik O., B. Holben, T. F. Eck, A. Smirnov, Y. J. Kaufman, M. D. King, D. Kino, D. Tanre, and I. Slutsker.. "Variability of absorption and optical properties of key aerosol types observed in worldwide locations", *J. Atm. Scie.* 59, 590-608 (2002).

8. Del Guasta M., M. Morandi, L. Stefanutti, B. Stein, and J. P. Wolf. C, "Derivation of Mount Pinatubo stratospheric aerosol mean size distribution by means of a multiwavelength lidar", *Appl. Opt*. 33, 5690–5697 (2002).

9. Wilkerson T.D., G. E. Bingham, V. V. Zavyalov, J. A. Swasey, J. J. Hancock, B. G. Crowther, S. S. Cornelsen, C. Marchant, J. N. Cutts, D. C. Huish, C. L. Earl, J. M. Andersen, and M. L. Cox, "AGLITE: A Multiwavelength Lidar for Aerosol Size Distributions, Flux and Concentrations of Whole Facility Emission**",** *Proceedings of the Workshop on Agricultural Air Quality: State of Science*, June 5-8, p.1238-1244 (2006).

10. Klett J. D, "Lidar inversion with variable backscatter/extinction ratio", *Appl. Opt*. 24, 1638-1683 (1985).

11. Dho S. W., Y. J. Park, and H. J. Kong, "Experimental determination of a geometrical form factor in a lidar equation for an inhomogeneous atmosphere", *Appl. Opt*. 36, 6009-6010 (1997).

12. Silva P. , R. S. Martin,V. Doshi, K. Moore, and M. Erupe, "Variations in Particle Composition and Size Distributions in and around a Deep Pit Swine Operation", *Proceedings of the Workshop on Agricultural Air Quality: State of Science*, June 5-8,584-585 (2006).

13. Hess M., P. Koepke, and I. Schult, "Optical Properties of Aerosols and Clouds: The software package OPAC", *Bull. Am. Meteorol. Soc*. 79, 831-844 (1998).

14. Jursa, A. S., *Handbook of Geophysics and the Space Environment,* Air Force Geophysics Laboratory, 1985.

15. Moon T. K., W. C. Stirling, *Mathematical Methods and Algorithms for Signal Processing*, Prentice-Hall, Inc., Upper Saddle River, New Jersey, 2000.

Downloaded From: http://proceedings.spiedigitallibrary.org/ on 04/02/2015 Terms of Use: http://spiedl.org/terms